

1           **Determination of erosion thickness by numerical back analysis:**  
2           **The case study of Badenian clays in the Carpathian Foredeep,**  
3           **Czech Republic**

4  
5 Richard Malát<sup>1</sup>, Josef Rott<sup>2</sup>, Monika Černíková<sup>3</sup>, Juraj Franců<sup>4</sup>, Jan Boháč<sup>5</sup> and David Mašín<sup>6</sup>

6  
7 <sup>1</sup> Faculty of Science, Charles University, Albertov 6, 12800 Prague, Czech Republic (malat@natur.cuni.cz)

8 <sup>2</sup> Faculty of Science, Charles University, Albertov 6, 12800 Prague, Czech Republic (rottj@natur.cuni.cz)

9 <sup>3</sup> Faculty of Science, Charles University, Albertov 6, 12800 Prague, Czech Republic  
10 (monika.cernikova@natur.cuni.cz)

11 <sup>4</sup> Czech Geological Survey, Leitnerova 22, 65869 Brno, Czech Republic (juraj.francu@geology.cz)

12 <sup>5</sup> Faculty of Science, Charles University, Albertov 6, 12800 Prague, Czech Republic (bohac@natur.cuni.cz)

13 <sup>6</sup> Faculty of Science, Charles University, Albertov 6, 12800 Prague, Czech Republic (masin@natur.cuni.cz)

14 **Abstract:** The paper describes an application of the geotechnical numerical back analysis in  
15 estimating the thickness of eroded sedimentary overburden in shallow basinal sediments. The  
16 approach is based on the back-analysis of the coefficient of earth pressure at rest  $K_0$  and on  
17 estimating the unloading from the obtained  $K_0$  value. This approach is compared with the  
18 conventional methods represented by Baldwin–Butler's “compaction curves” and Casagrande's  
19 concept of “preconsolidation stress”. The results of these two commonly used methods are  
20 incorrect if the sedimentary profile is affected by “ageing” effects, such as cementation,  
21 secondary compression etc. The method is demonstrated on the Lower Miocene marine clay,  
22 often called „Tegl” which was deposited in the Carpathian Foredeep in the vicinity of Brno,  
23 Czech Republic. The numerical back analysis was applied to galleries and adits opened during  
24 site investigation of the Královo Pole Tunnels in Brno. The application of Baldwin–Butler's  
25 equation suggested the erosion thickness of 180-270 m and Casagrande's method of 100–  
26 800 m, while the numerical back analysis of 0–40 m.

27  
28 **Key words:** ageing, coefficient of earth pressure at rest, compaction curve, erosion thickness,  
29 numerical back analysis, Tegl

## 30 **1. Introduction**

31 The thickness of erosion of sediments can be estimated using purely geological approach  
32 determining the altitudes of the current surface of the stratum and its denudation relics. An  
33 essential disadvantage of this approach is the fact that the result can be significantly affected by  
34 tectonic (vertical) movements. In order to avoid the problem, several techniques based on  
35 analyses of the mechanical properties of the soils have been developed. But it is well known  
36 that most mechanical properties of soils change during ageing (e.g., Chandler, 2010, Mesri and  
37 Hayat, 1993). The ageing effects are difficult, or impossible to quantify, and invalidate the  
38 estimates of the erosion thickness. This also disqualifies the two most common methods based  
39 on the analysis of mechanical properties: Baldwin–Butler's equation (1985) and Casagrande's  
40 method (1936).

41 Determining the erosion thickness by the proposed geotechnical numerical back analysis does  
42 not have to consider the ageing effects, which would be necessary in both Casagrande's and  
43 Baldwin - Butler's method. On the other hand, the procedure assumes that there is no change  
44 in horizontal stress due to ageing. The literature review, however, revealed that the effects of  
45 ageing on the horizontal stress (and  $K_0$ ) in clay massifs has not been solved to date. Nevertheless  
46 assuming constant horizontal stress seems to be plausible (Holtz and Jamiolkowski 1985,  
47 Gareau et al., 2006). In the following, the results of a numerical back analysis are compared  
48 with Baldwin–Butler's and Casagrande's methods.

49 A soil affected by ageing had to be chosen for such a study. The Miocene clay of the town of  
50 Brno called “Tegl” seemed a good candidate for such an exercise: it had clearly been subjected  
51 to ageing since its sedimentation in the Carpathian Foredeep, and its thickness of erosion is still  
52 a matter of dispute. The estimated values vary from tens to hundreds of metres (e.g., Boháč  
53 and Pavlová, 2012, Pavlík et al., 2009). Moreover, a well-documented geotechnical case-history  
54 was available for the study – the Královo Pole Tunnels project, during which exploratory adits,

55 drifts, and final motorway tunnels were excavated in the Tegl strata (Pavlík et al. 2004, Svoboda  
56 et al., 2009; 2010).

## 57 **2. Geological setting**

58 The analyses were made on Middle Miocene, Early Badenian calcareous clayey sediment in  
59 the Carpathian Foredeep, further referred to Tegl. The Early Badenian (Moravian) sediments  
60 of the Carpathian Foredeep basin were deposited during a marine transgression from the ESE  
61 on the East margin of the Bohemian Massif. The lowermost units include the Iván Beds and  
62 basal Brno sandstones and conglomerates with local maximum thickness of 190 m (Stráník et  
63 al., 2016). They are overlain by deepwater fine grained sediments described as Tegl. This unit  
64 without a formal lithostratigraphic name consists of blue-, brown- to green-grey massive  
65 calcareous clay with sandy laminae and horizons in the lower part. Frequent lenticular bodies  
66 are enriched in organic matter and fragments of molluscan shells. Tegl onlaps on the pre-  
67 Neogene units in the West and widely surpasses the regional extent of the basal clastics. This  
68 transgression is correlated with the eustatic sea level rise of the global ocean and the paleo-  
69 water depth is estimated to be as high as 100 m West of Brno city while 200-500 metres in  
70 upper bathyal setting in Brno-Královo Pole (Brzobohatý, 1982). Radiometric measurements of  
71 rhyodacite tuffs and tuffitic clays, which occur in local interlayers, provide age estimation of  
72  $16,2 \pm 2,1$  mil. years (Nehyba, 1997). The maximum known thickness of Tegl is more than  
73 1000 m East of Ostrava city.

74 Tegl consist typically of quartz (ca 29%) and calcium carbonate (ca 31%). Smectite was  
75 detected only at small amounts (ca 3%). Gypsum and pyrite are also encountered in Tegl. Fe  
76 hydroxides in Tegl are products of the process of the gradual oxidation of pyrite. Calcium  
77 carbonate is present in form of the crystalline (calcite  $\text{CaCO}_3$ ). The amorphous form of the  
78 calcium carbonate that could cause the cementation is not present, because the calcite

79 precipitation from the solutions during post sedimentation process does not support formation  
80 of the amorphous form.

81 It is obvious that the top of the deepwater Early Badenian is erosional and that younger  
82 sediments which covered Tegl have been removed. The strata are influenced by ageing effects,  
83 such as secondary compression (Boháč and Pavlová, 2012) or tectonic movements (Pavlík  
84 2004). The thickness of the eroded units has not been estimated in a satisfactory manner up to  
85 now.

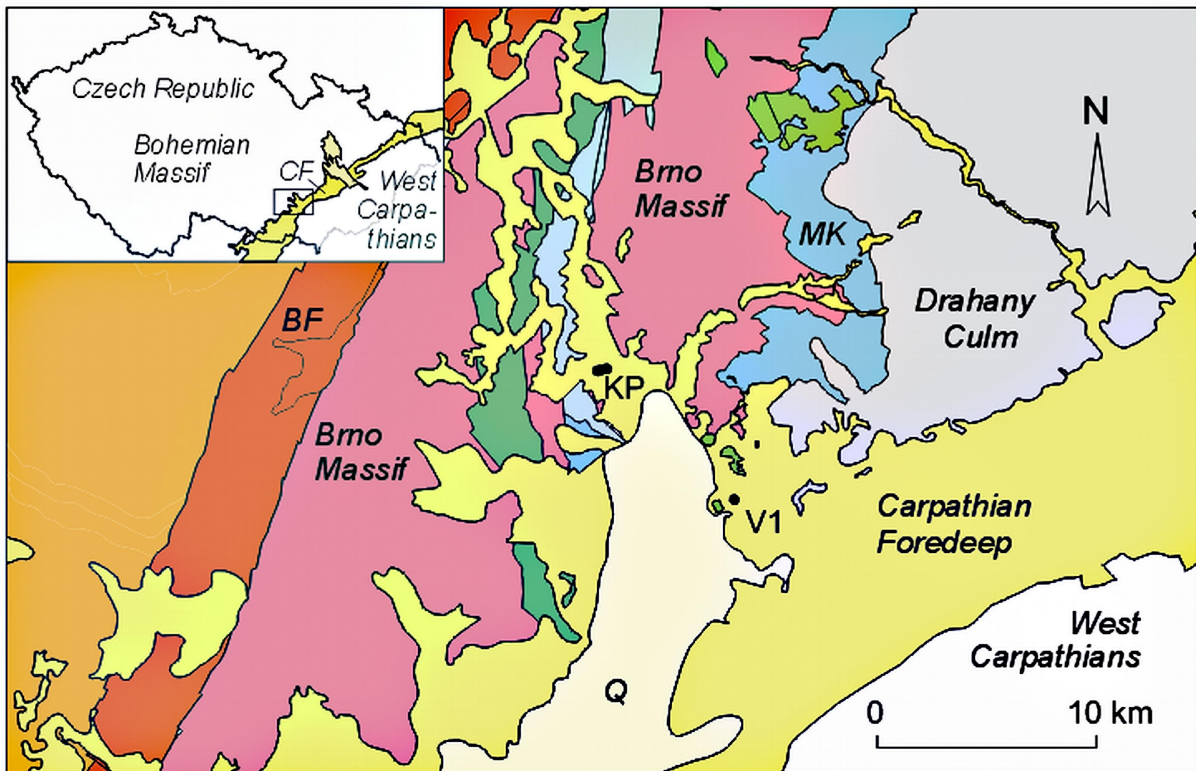
### 86 **3. Investigated sites**

87 Samples and data from two sites in the area of Brno town were used. Data from Brno - Královo  
88 Pole (Královo Pole Tunnel project) were used in the numerical back analysis. After completion  
89 of Královo Pole tunnels, however, obtaining of new undisturbed samples of Tegl was  
90 impossible in the developed area. The samples for analyses according to Baldwin - Butler's and  
91 Casagrande's proposals were therefore taken from Brno - Slatina (position of the V1 borehole  
92 in Fig.1). The thickness of erosion of Tegl for both site is assumed to be the same or very similar  
93 due to several reasons:

94 1) No significant tectonical movement has been identified between the areas.

95 2) The current head of the Tegl stratum is approximately at the same level at both sites (ca 230  
96 - 245 m above sea level).

97 3) The coastline of the sea during depositing of the stratum is estimated to be 15 – 30 km from  
98 the investigated sites and that is why horizontal surface of Tegl after depositing is assumed for  
99 both sites.



100

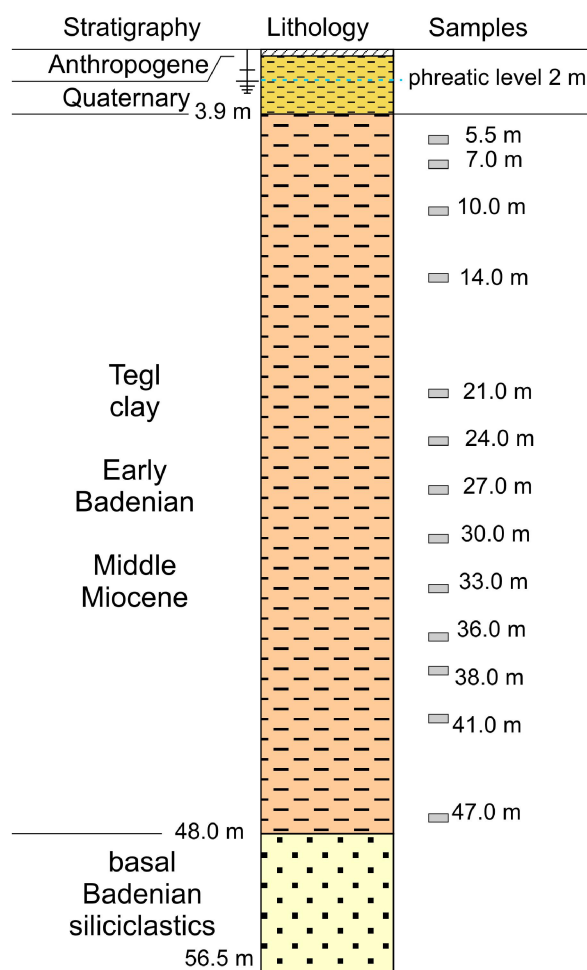
101 *Fig. 1. Locations of KP (Královo Pole tunnel) and V1 (Brno Slatina) boreholes. The yellow area shows the*  
 102 *extension of the Carpathian Foredeep, adjacent geological units are shown for reference.*

103 **3.1 V1 borehole**

104 The borehole V1 was situated in Brno town between Drážní and Šmahova streets. Coordinates  
 105 of the axis of the borehole are: 49.1709261N, 16.6826475E (WGS). The surrounding is flat and  
 106 reaches approx. 250 m above sea level. Quaternary sediments are encountered in relatively thin  
 107 layers (up to first metres) and thickness of Tegel is assumed several tens metres according to  
 108 available archival data.

109 A spiral drillbit in dry drilling mode was used and the depth of 56.5 m was reached. Every ca  
 110 three metres, undisturbed samples were taken using a pushed-in thin-walled steel sampler. The

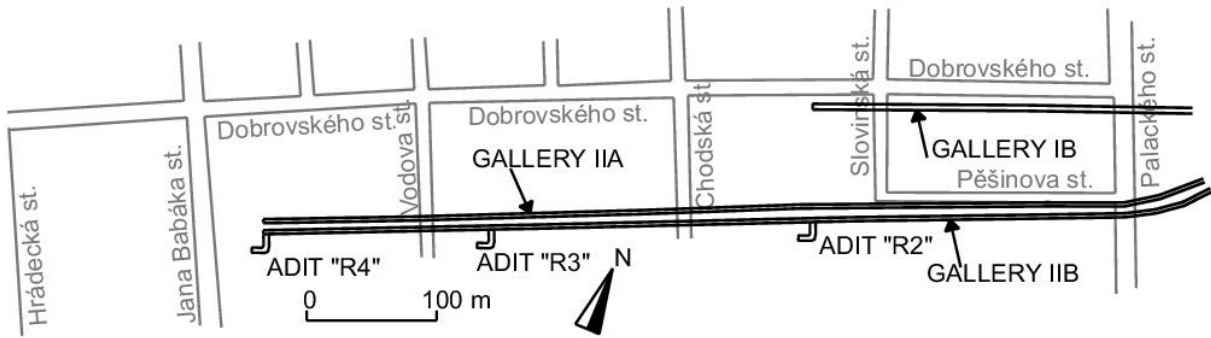
111 V1 profile (Fig. 2) consists of anthropogenic debris at depth of 0-0.5 m and Quaternary eolian  
 112 and deluvial silts and clays at 0.5-3.9 m. Early Badenian Tegl fills the 3.9-48 m interval, with  
 113 grey-brown clay at depth of 3.9-13.8 m gradually changing into a layer of non-weathered and  
 114 very stiff grey-green clay at 13.8-19.5 m. Basal Lower Badenian grey-green clayey sand and  
 115 gravel were encountered at 48.0-56.5 m.



116  
 117 *Fig. 2. Schematic profile of V1 borehole with marked position of undisturbed samples.*

### 118 3.2 Královo Pole Tunnels

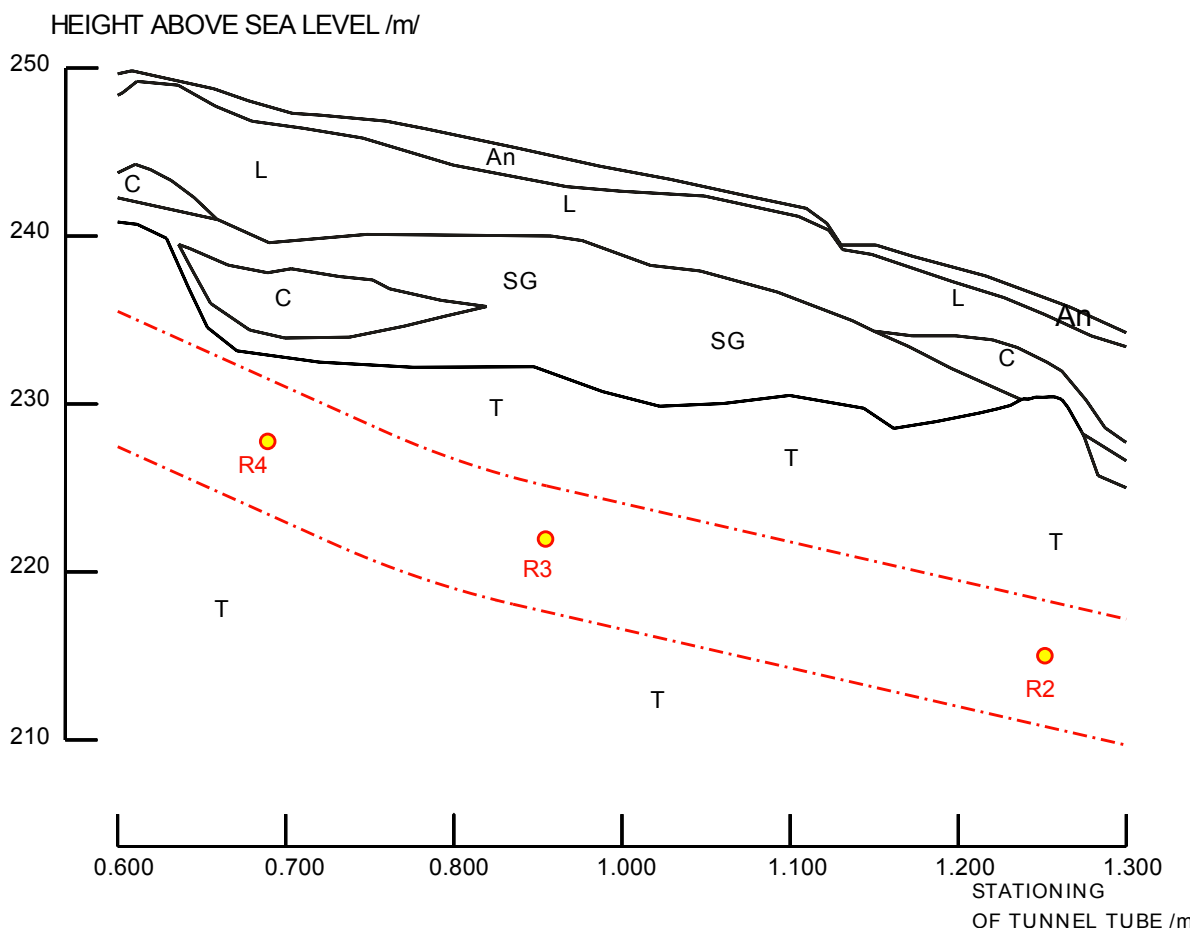
119 The two two-lane road tunnels of the Královo Pole project are situated in the north-western part  
 120 of Brno. Three exploratory galleries and four adits were excavated, instrumented and monitored  
 121 as a part of the site investigation (Fig. 3). Geological setting around exploratory galleries is  
 122 presented in Fig. 4. Head of Tegl stratum above the adits is approximately 230 m above sea  
 123 level. Quaternary sediments above Tegl clay consist mainly of loess and fluvial sand and gravel  
 124 (see Pavlík et al. 2004 for detailed information).



125

126 *Fig. 3. Underground works during Královo Pole Tunnels site investigations – Exploratory galleries and*  
 127 *unsupported adits (Pavlík et al. 2004).*

128



129

130 *Fig. 4 Geological setting around analyzed adits. T – Tegl clay, SG – sand with gravel, C – clayey silt, L – loess,*  
 131 *An – anthropogenic sediments. Tunnel tube is marked with dot-and-dash lines.*

## 4. The thickness of erosion determined by conventional methods

### 4.1 Baldwin–Butler's equation

An empirical equation for the burial depth  $b_d$  was proposed by Baldwin and Butler (1985) which is a regression curve of data collected mainly by Baldwin (1971) and several other authors. The equation is valid for argillaceous sediments.

$$b_d = 6.02 S^{6.35} \cdot 1000 \text{ [m]} \quad (1)$$

where solidity  $S$  [%] is the volume of solid grains as a percent of total volume of sediment; it is a complementary value to porosity  $n = (100-S)$  [%.]

The porosity (solidity) of a sample changes after removal from the *in-situ* stress conditions. In the laboratory, for estimation of solidity the samples have to be reconsolidated to the *in-situ* effective vertical stress  $\sigma'_v$ :

$$\sigma'_v = \gamma_{sat} \cdot h - u \text{ [kPa]}$$

(2)

where

$\gamma_{sat}$  – [kN.m<sup>-3</sup>] unit weight of fully saturated soil,

$h$  – [m] overburden height,

$u$  – [kPa] pore pressure *in-situ*

The unit weight  $\gamma_{sat}$  of Tegl of 18.8 kN.m<sup>-3</sup> (Svoboda et al. 2009, 2010) was used.

The thickness of erosion is then calculated simply from the depth of burial and the depth of sampling under current surface:

$$E = 6.02 S^{6.35} \cdot 1000 - h \quad (3)$$

$E$  – [m] thickness of erosion.

#### 4.1.1 Results and discussion

The thickness of erosion calculated according to Baldwin-Butler's equation is summarized in Tab. 1. It is obvious that the values fluctuate around approximately 200 m, with the maximum



157 and minimum values of 245 and 177 m, respectively. However, ageing is not accounted for in  
 158 the Baldwin-Butler's equation. Moreover, the increase of porosity due to unloading by erosion  
 159 is neglected.

160  
 161

*Tab. 1. Erosion thickness calculated using Baldwin–Butler's equation.*

Depth sampling (current burial) [m]	Solidity „S“ after reconsolidation [%]	Calculated erosion thickness [m]
7	59,4	<b>214</b>
14	59,7	<b>213</b>
21	67	<b>231</b>
24	59,9	<b>208</b>
27	61,2	<b>240</b>
30	61,3	<b>240</b>
33	59,7	<b>193</b>
36	59,9	<b>195</b>
38	59,2	<b>177</b>
41	61,9	<b>245</b>
47	61,5	<b>227</b>

162

#### 163 **4.2 Casagrande's method**

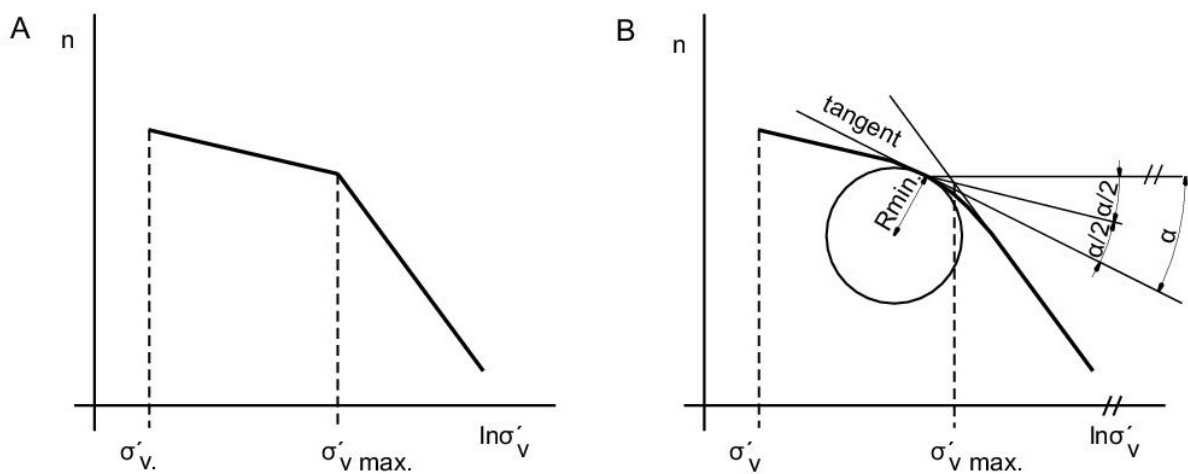
164 Casagrande (1936) stated that the largest overburden under which the soil (clay) had once been  
 165 consolidated can be determined as the “pre-consolidation load” in the one-dimensional  
 166 compression test in the oedometer. Further he suggested a graphical method of determining the  
 167 value of the preconsolidation pressure  $\sigma'_{v \max}$  from the oedometer test results. An ideal  
 168 compression curve of a preconsolidated (overconsolidated) sediment is shown in Figure 5A.  
 169 For a real sediment however, with the compression curve not showing a clear kink of the  $n$ -  
 170  $\log\sigma'_v$  curve, the preconsolidation pressure is determined as shown in Fig. 5B. The method is  
 171 often used to date, despite the fact that original Casagrande's geological interpretation must be  
 172 in error due to ageing. However, neglecting ageing and provided the weight of the sediment is  
 173 known, it is tempting to determine erosion thickness for soils sedimented in water from

$$174 \quad E = \frac{\sigma'_{v \max}}{(\gamma_{sat} - \gamma_w)} - h \text{ [m]} \quad (4)$$

175  $\sigma'_{v \max}$  – [kPa] preconsolidation pressure

176  $\gamma_w$  – [kN.m<sup>-3</sup>] unit weight of water

177 The undisturbed samples from the borehole V1 were subjected to one-dimensional oedometer  
178 compression. After reconsolidation to the estimated *in-situ* vertical stress the incremental step-  
179 wise loading was applied to the vertical stress of about 10 MPa (Fig. 7), which is substantially  
180 higher than the values suggested for overconsolidated and stiff clays in practice (Head and  
181 Epps, 2011). Despite the elevated stress levels the determination of preconsolidation pressure  
182 by Casagrande's method proved difficult. The results are in Table 2.



183

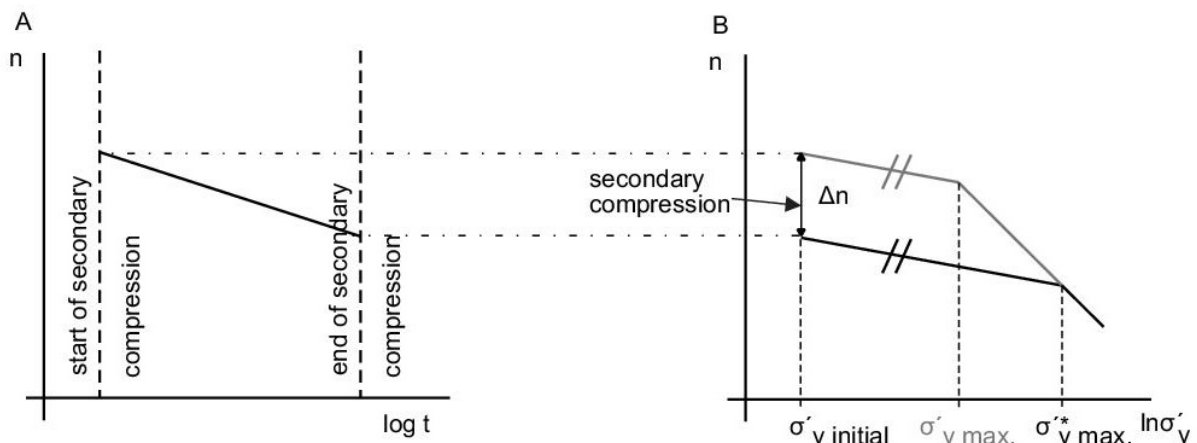
184 Fig. 5. Semilogarithmic oedometer compression curve in the plane of porosity and vertical pressure  $\ln\sigma'_v$ : A) An  
185 idealised oedometer compression curve; B) Determination of  $\sigma'_{v\max}$  proposed by Casagrande (1936).

186 As suggested above, Casagrande's geological interpretation of preconsolidation pressure is in  
187 error due to ageing, namely due to reduction of voids portion during time.

188 Decreasing of porosity without a change in vertical effective pressure is pronounced especially  
189 with clays. Due to secondary compression, oedometer tests carried out on good quality  
190 specimens of natural clay inevitably determine a “quasi-preconsolidation pressure”  $\sigma'^*_{v\max}$   
191 instead of the “true” preconsolidation pressure  $\sigma'_{v\max}$  (Leonards and Altschaeffl, 1964; this is  
192 also included in Bjerrum's (1967) “delayed consolidation” and the concept of “time lines”). The  
193 quasi-preconsolidation pressure  $\sigma'^*_{v\max}$  determined by Casagrande's method can reach  
194 substantially higher value than the true preconsolidation pressure  $\sigma'_{v\max}$  (Fig. 6).

195 The change in porosity during secondary compression may be estimated using the secondary  
 196 compression index  $C_\alpha$  [-]. In geotechnical practice  $C_\alpha$  is determined as the slope of the linear  
 197 portion of the compression curve plotted as voids ratio vs logarithm of time (e.g., Head and  
 198 Epps, 2011). However the extrapolation to geological times is a very crude and questionable  
 199 estimate.

200



201

202 *Fig. 6. Definition of secondary compression (A), and its influence on the compression curve (B).*

203 Further, in order to estimate the change of porosity during secondary compression, it is  
 204 necessary to determine its duration. The time needed for the sedimentation of the Tegl strata  
 205 encountered in the V1 borehole was assessed by magnetostratigraphic measurements on the  
 206 undisturbed samples (Bosák and Pruner, 2014), which showed that the sedimentation took place  
 207 approximately between 14.8 and 14.24 Ma before present. The rate of sedimentation was so  
 208 slow that the older part of the stratum was affected by secondary compression when the younger  
 209 part of the stratum had not been sedimented yet. Hence, we decided to consider the mid-point  
 210 of the sedimentation (14.52 Ma before present) for our calculation.

211

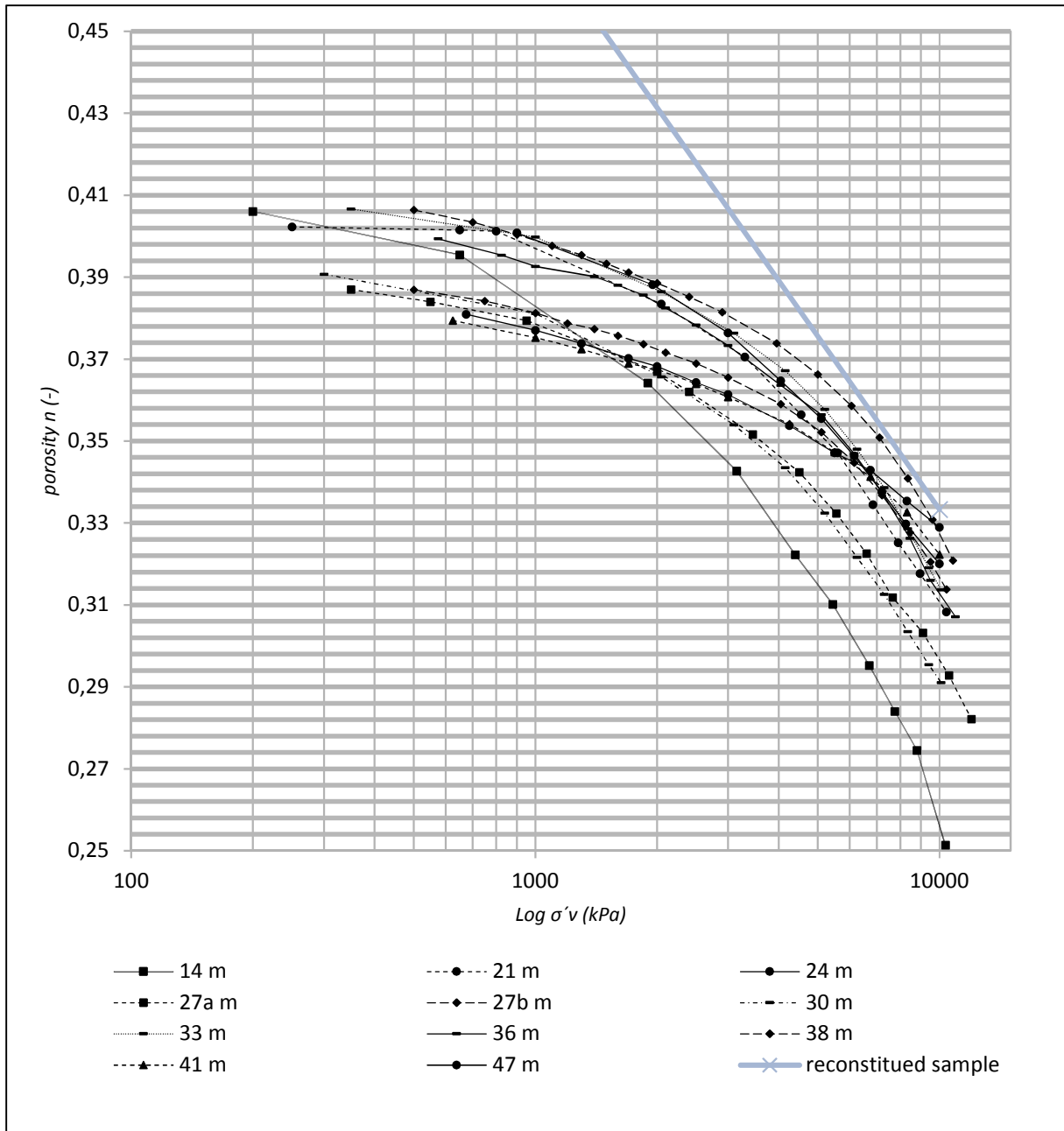
#### 212 **4.2.1 Results and discussion**

213 Applying the value of  $C_\alpha = 0.016$  (Boháč and Pavlová, 2012) to the samples from the borehole  
 214 V1, the decrements  $\Delta n$  of porosity during secondary compression and consequently the  
 215 corresponding thicknesses of erosion were calculated from the laboratory compression curves

216 of Fig. 7 (Table 2). A test on reconstituted sample was carried out in order to evaluate the curves  
217 of undisturbed samples according to Casagrande's approach (see fig. 7).  
218 The obtained thicknesses of the eroded layer vary between 134 – 766 (approx. 100 – 800 m)  
219 Thus, the results cannot be considered reliable.

220 The problem of Casagrande's proposal to use the oedometer test in studying the overburden  
221 pressures in the geological history was well expressed by Mayne and Kulhawy (1982): “At  
222 present, however, there appears to be no known technique of determining  $OCR_{max}$  ...” (i.e. true  
223 preconsolidation pressure) “...for a specific soil deposit other than a good knowledge of local  
224 geology and stress history of the soil deposit.” The skepticism of the quotation is clearly  
225 confirmed by the discussion of our data above. Burland (1990) or Chandler (2010) also point  
226 out the problem explicitly, however, Casagrande's (1936) approach is still the most used  
227 technique for  $OCR$  (or quasi -  $OCR$ ) determination. It has to be mentioned that alternative  
228 methods for estimation of  $\sigma'_{v\ max}$  from oedometer test has been suggested (e.g., Jefferies et al.  
229 1987). Nevertheless, this is a technique for better determining of the „kink point“ and do not  
230 deal with the fact that the point does not respond to true overconsolidation pressure in the case  
231 of aged soils.

232 These facts served as motivation for proposing the new approach in the next chapter: combining  
233 a numerical geotechnical model with the well-established empirical relationship between in-  
234 situ stresses ( $K_\theta$ ) and the true preconsolidation pressure (i.e.  $OCR_{max}$ ) due to Mayne and  
235 Kulhawy (1982).



236

237 *Fig. 7. Compressibility curves from oedometer tests on undisturbed specimens of V1 borehole.*

238

239

240

241

242

243

244

Tab. 2. The thickness of erosion of Tegl determined using oedometer tests.

Sample No.	depth of the samples [m]	$\sigma'_v$ [kPa]	$\Delta n$ [-]	$\sigma'^*_{v \max}$ [kPa]	$\sigma'_{v \max}$ [kPa]	thickness of erosion [m]
4	14	124	066	2100	1300	<b>134</b>
5	21	185	053	3950	2600	<b>274</b>
6	24	211	047	5400	4050	<b>436</b>
7	27	238	035	7050	5550	<b>604</b>
8	30	264	055	3900	2300	<b>231</b>
9	33	290	050	5000	3450	<b>359</b>
10	36	317	048	4850	2700	<b>271</b>
11	38	334	046	5050	4000	<b>417</b>
12	41	361	031	8950	7100	<b>766</b>

## 246 5. The thickness of erosion estimated by geotechnical numerical back 247 analysis

248

249 Our geotechnical numerical back analysis simulated the mechanical behaviour of the  
250 underground excavations carried out during the Královo Pole Tunnels project. As the project  
251 was relatively complex, the readers are referred to another publication for more details on the  
252 modelling procedure (Rott et al., 2015). The project consisted of two road tunnels, supported  
253 exploratory galleries of triangular cross-sections and unsupported four adits of circular cross-  
254 section, which all were thoroughly monitored. For our analysis, the unsupported adits were the  
255 most important. They were excavated from the exploratory gallery and they were intentionally  
256 left without any active support to make it possible to measure the convergence (“squeezing”)  
257 of the cavities. Back-calculating the measured “squeezing” of the cavities by optimization of  
258 the value of the coefficient of earth pressure at rest  $K_0$  using an appropriate advanced numerical  
259 model (Mašín, 2014; Rott and Mašín, 2014) allowed us to obtain the *in-situ* stress state in the  
260 clay massif prior to the excavation works. Knowing the *in-situ* stresses, which in the case of  
261 over-consolidated stiff clays are believed the most difficult parameters to be obtained (e.g.,  
262 Hight et al., 2003), the depth of erosion could be calculated with a reasonable confidence. In  
263 the subsequent text, this procedure is explained in more detail.

264 **5.1 Initial stresses in the numerical model**

265 The initial *in-situ* stresses must be put into the advanced numerical models to simulate correctly  
266 excavations, typically using  $K_0$

267 
$$K_0 = \sigma'_h / \sigma'_v \quad [-] \quad (5)$$

268 where

269  $\sigma'_v$  and  $\sigma'_h$  are the vertical and horizontal effective stresses, respectively.

270  $K_0$  depends on the stress history of the soil, as was proved by a number of laboratory  
271 measurements (e.g. Brooker and Ireland, 1965, or Mayne and Kulhawy, 1982). The latter  
272 authors suggested an empirical equation, derived from laboratory data of loaded-unloaded-  
273 reloaded specimens of both sands and clays. This type of test is a laboratory simulation of  
274 sedimentation-erosion-redeposition process:

275 
$$K_0 = (1 - \sin\phi') \left[ \frac{OCR}{OCR_{max}^{(1-\sin\phi')}} + \frac{3}{4} \left( 1 - \frac{OCR}{OCR_{max}} \right) \right] \quad (6)$$

276 where  $\phi'$  is critical state friction angle of the soil (the critical state – see, e.g., Atkinson,  
277 2007) and  $OCR$  is the overconsolidation ratio, defined as the ratio of the maximum and  
278 current vertical effective stresses:

279 
$$OCR_{max} = \sigma'_{vmax} / \sigma'_1 \quad [-] \quad (7)$$

280 
$$OCR = \sigma'_{vmax} / \sigma'_2 \quad [-] \quad (8)$$

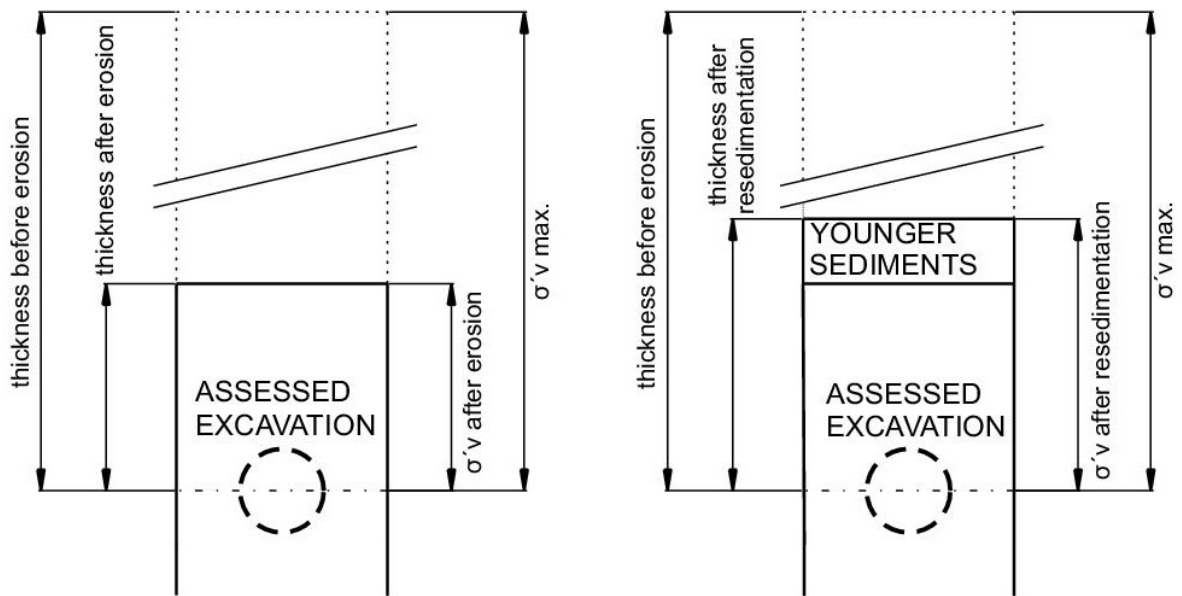
281  $\sigma'_1$  = stress after erosion;  $\sigma'_2$  = stress after redeposition

282

283 It is important to note that (6) is valid only for mechanical loading, unloading and re-loading of  
284 soils, i.e. true preconsolidation. It means that if  $\sigma'^*_{vmax}$  is used the result is not correct.

285 Therefore the equation (6) might not be used in estimating the stresses for Královo Pole  
 286 Tunneling project directly from undisturbed oedometer specimens. However, if the stress state  
 287 is reliably determined by another method – in our case by iterative back analysing the  $K_0$  from  
 288 the measured squeezing of the adits – the equation (6) can be used for calculating the thickness  
 289 of erosion (under the assumption of constant  $K_0$  during ageing, see the discussion later).

290



291

292

Fig. 8. Effective vertical stress of equations (7) and (8).

293 Thus, geotechnical numerical back analysis consist of several steps:

294

1)  $K_0$  found by trial-and-error method in numerical model

295

2) Determining appropriate  $\sigma'_{v \max}$  in order to obtain  $OCR$  and  $OCR_{\max}$  which give the same  
 296 value of  $K_0$  as in the step 1) according to Eq (6)

297

3) Erosion thickness is computed using Eq (4).

298

## 299 5.2 Description of the model

300

The three modelled unsupported adits R2, R3 and R4 were excavated perpendicularly to the

301

exploratory gallery IIB (Fig 3 and 4). They had a circular cross-section of approx. 2 metres in

302

diameter. The steel frames (Fig. 9) were installed for the sake of security only, and they were



303 not in contact with the face of excavation, and there was no need to consider them in the  
304 numerical model.

305  
306



307

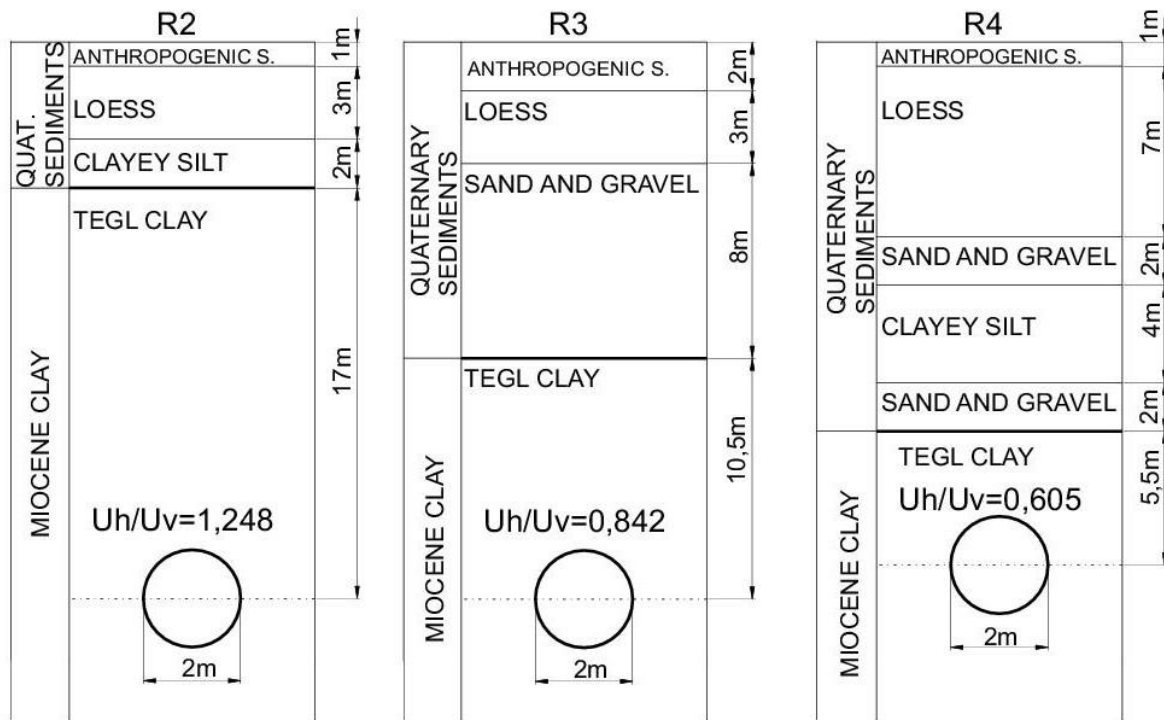
308 *Fig. 9. Lining with the offset of 50 mm from the soil (adit R2; photo by J. Pavlík).*

309 The hypoplastic constitutive model (Mašín, 2005) augmented with inherent anisotropy was  
310 used for Tegl. It allows for different stiffnesses in the horizontal and vertical directions (Mašín  
311 and Rott 2014, Mašín, 2014), which is a crucial requirement for simulating the squeezing of the  
312 adits properly.

313 The geological conditions of the three adits were determined by the geological and geotechnical  
314 site investigations for Královo Pole Tunnels (Pavlík et al., 2004), and they have been simplified  
315 for the purpose of the geotechnical model (see Fig. 10). The ground water level was situated at  
316 the interface of Quaternary sediments and Miocene Tegl.

317 Determination and calibration of the model parameters of the soils are out of the scope of the  
318 present paper, and the reader is referred to Rott et al. (2015).

319  
320

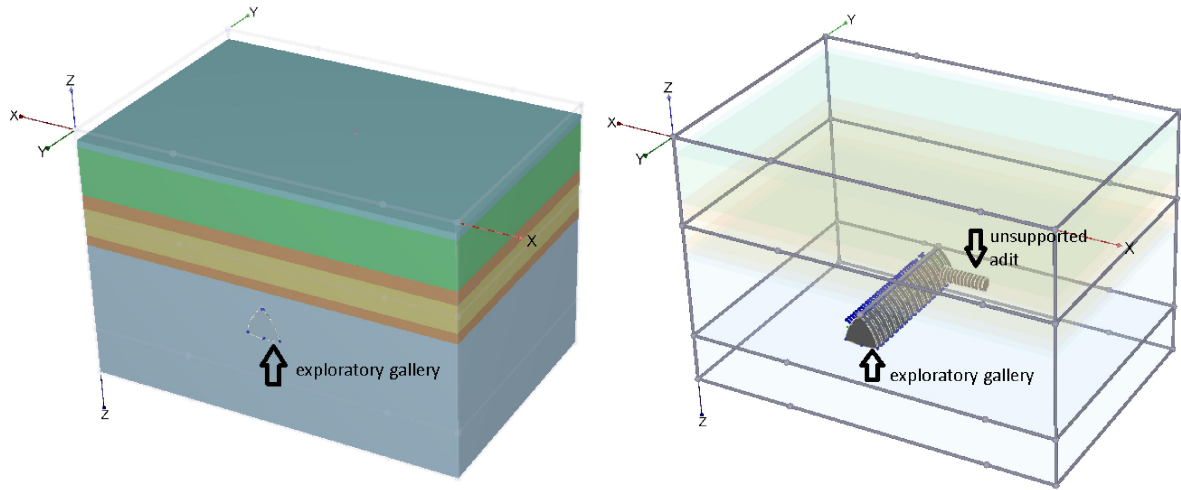


321

322 *Fig. 10. Geological conditions of the adits and the ratio of horizontal ( $U_h$ ) and vertical ( $U_v$ ) deformations*  
 323 *measured in the modelled convergence profiles.*

324 The adits were modelled in three dimensions by finite elements (FEM) using the commercially  
 325 available geotechnical software Plaxis 3D. The model was 55 m wide, 37 m deep and 36 m  
 326 long. Since the studied “convergence profiles” in the adits were just a few metres from the  
 327 exploratory gallery, each model contained both the adit and the gallery (Figs. 11 and 12).

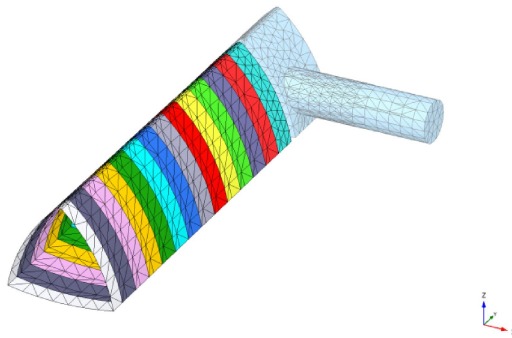
328 The primary lining of the gallery has been composed of two components: the shotcrete and a  
 329 massive steel support. The lining has been modelled using shell elements characterised by a  
 330 single parameter set obtained using homogenisation procedure described in Rott (2014).



331  
332

Fig. 11. 3D model of the unsupported adit and the exploratory gallery in Plaxis software.

333



334

335 Fig. 12. Junction of the exploratory gallery and the unsupported adit. Different colours indicate excavation steps,  
336 each associated with different time-dependent lining stiffness.

337 As suggested above, the aim of the numerical modelling was to obtain by  $K_0$  optimization the  
338 same ratio of horizontal ( $U_h$ ) and vertical ( $U_v$ ) displacements, which was measured *in-situ* for  
339 3 adits R2, R3, R4.  $K_0$  was changed repeatedly by trial-and-error until the model convergence  
340 approximately equalled the monitored values (Boháč et al., 2013). In the cavity R2 the ratio of  
341 the deformations was  $U_h/U_v = 1.248$  In the case of the R3 and R4 cavities the ratios were  $U_h/U_v$   
342  $= 0.842$  and  $U_h/U_v = 0.605$ , respectively (Table 3).

343 In the final step, Equation (6) was used to find the overburden stresses, and thus the depths of  
344 erosion, corresponding to the values of  $K_0$  determined by the 3D numerical modelling. For this  
345 purpose, the geological development of the investigated site was simplified in the following

346 way: the sedimentation of Tegl took place under water, and all the time during erosion the water  
 347 level coincided with the surface of Tegl. Second, the Quaternary sediments of constant  
 348 (current) thickness were considered. Last, similarly to Casagrande's method, constant unit  
 349 weight of Tegl of  $18.8 \text{ kNm}^{-3}$  was assumed, regardless of the depth below the surface.

#### 350 5.4 Results and discussion

351 Tab. 3 shows the deformation ratios measured *in-situ*, the deformations obtained by the  
 352 numerical model after the optimisation procedure, and the corresponding  $K_0$  values of the 3D  
 353 model for the individual adits.

354 *Tab. 3. Convergence ratios and corresponding values of  $K_0$ .*

Adit	$U_h/U_v$ measured <i>in-situ</i>	$U_h/U_v$ from the models after $K_0$ optimization	Corresponding $K_0$
R2	1.248	1,250	<b>0.75</b>
R3	0.842	0.842	<b>0.58</b>
R4	0.605	0.601	<b>0.60</b>

355  
 356 Tab. 4 shows the computed  $K_0$  coefficients with respect to the current thicknesses of Tegl from  
 357 the centres of the adits to the top of Tegl (base of Quaternary). Furthermore, Tab. 4 shows  $K_0$   
 358 values given by the equation (6) for arbitrarily chosen thickness of erosion.

359 *Tab. 4. Comparison of the  $K_0$  values of the 3D model analyses and those calculated using equation (6)*

Adit	Thickness of the Tegl strata/m/	Thickness of Quaternary strata /m/	$K_0$ from numerical back analysis /-/	$K_0$ /-/ from Eq. (6) for erosion:		
				0 m	20 m	40 m
R2	17	6,0	75	0.63	0.68	0.76
R3	15	13.0	58	0.63	0.63	0.70
R4	5.5	16.0	60	0.63	0.63	0.69

360  
 361 The numerical back analysis combined with the empirical equation for  $K_0$  suggested that the  
 362 erosion of Tegl at Královo Pole was between 0 to 40 metres. However, the  $K_0$  values obtained  
 363 by the advanced numerical analyses for the adits R3 and R4 are slightly lower than for the

364 normally consolidated (0 m erosion) Tegl. The discrepancy could be caused by several reasons,  
365 which are discussed in the following.

### 366 **Uncertainty in input parametres**

367 The presented numerical back analysis depends on many geotechnical parametres and state  
368 variables. The most important mechanical phenomena influencing the results however are the  
369 inherent anisotropy (Mašín and Rott, 2014; through its effect on the results of the numerical  
370 back-analysis) and the soil strength (through its effect on estimating the erosion from the value  
371 of  $K_\theta$ ).

372 The critical state friction angle is a function of mineralogy and grading. The Tegl strata are not  
373 consisting of pure clay fraction, and locations with, for example, a substantial amount of sand  
374 particles occur. They have an inevitable influence on the critical state strength expressed by  $\phi$   
375  $'$ . The previously published values for Tegl from several locations ranged between approx. 19  
376 and 27 degrees (Svoboda, 2009, Boháč, 1999). The significant role of the friction angle in  
377 estimating the erosion thickness is clear when Eq. (6) is inspected. The coefficient  $(1-\sin\phi')$  in  
378 Eq. (6) is 0.67 for  $\phi'=19^\circ$  and 0.55 for  $\phi'=27^\circ$ . We adopted  $\phi'=22^\circ$  as the most credible value,  
379 determined by triaxial test on specimens from the vicinity of the adits.

380 The inherent anisotropy was expressed as the ratio " $\alpha_G$ " of horizontal and vertical moduli of  
381 the soil and in the model the ratio was assumed a constant:  $\alpha_G = 1.45$ . For adit R2 the  
382 dependence of  $K_\theta$  on  $\alpha_G$  was evaluated by Rott et al. (2015), and the result is presented in Fig.13.  
383 *In-situ*, soils may be influenced by several other factors, for example tectonic movements,  
384 diagenesis etc., which can cause spatial inhomogeneity of stiffness. This has already been  
385 proved for Tegl by *in-situ* measurement (Malát et al., 2015).

386 Considering the inherent uncertainties in the parametres and of the model, and the relatively  
387 small differences in  $K_\theta$  values obtained (Table 4) the thickness of erosion of 20 to 40 metres is  
388 believed to be a plausible estimate.

389

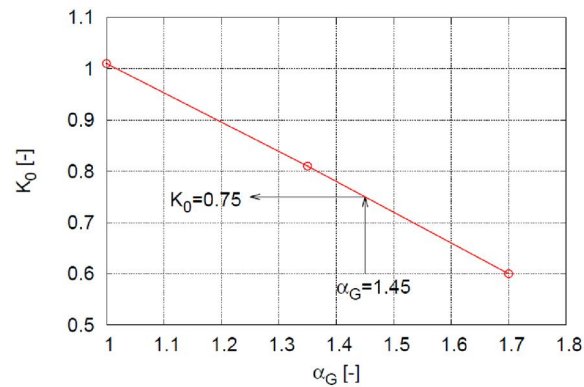


Fig. 13.  $K_0$ - $\alpha_G$  relationship for R2 adit (Rott et al. 2015).

390  
391  
392

### 393 Simplification of geological development

394 Closer to the surface  $K_0$  is relatively more responsive to change in effective stress since related  
395  $OCR$  change is higher in comparison with deeper part of a stratum. Cyclic erosion and re-  
396 deposition of Quaternary sediments or ground water level fluctuation even in range of a few  
397 metres affect  $K_0$  significantly in upper part of Tegl clay. Moreover, the upper part of Tegl strata  
398 can be remoulded by climatic influences which can result in “loss” of overconsolidation. It is  
399 impossible to reconstruct the evolution of the geological basin completely. Hence, it seems  
400 plausible to consider the model and result of adit R2 more relevant, since the Tegl overburden  
401 is the thickest.

### 402 Assumption of constant $K_0$ during ageing

403 The numerical back analysis was based on the assumption that  $K_0$  does not change during  
404 ageing. However the influence of ageing on  $K_0$  is still a matter of dispute in the geotechnical  
405 literature.

406 The most discussed phenomena is the influence of the secondary compression on  $K_0$ . Several  
407 laboratory studies have been carried out with different results (Mesri and Hayat, 1993,  
408 Kavazanjian and Mitchell 1984, Gareau et al., 2006). The discrepancy is caused probably by  
409 the problem that during the tests zero horizontal strain has to be kept. Some of the older  
410 laboratory test supported the opinion that  $K_0$  due to secondary compression gradually converges  
411 towards the value of 1.0 (e.g. Kavazanjian and Mitchell, 1984) but their conclusions have been

412 criticized for unacceptable strains compensated during the tests (Holtz and Jamiolkowski,  
413 1985). Others showed (e.g. Mesri and Hayat, 1993) that  $K_0$  during secondary compression  
414 increases. Some newer laboratory data, however, that the  $K_0$  was constant with time (Gareau et  
415 al., 2006). Construction of their device allowed the smallest strains of a soil in comparison with  
416 the older devices. Hence, in our model we assumed that  $K_0$  is constant.

417 Apart from secondary compression other ageing effects are difficult to quantify. Nevertheless,  
418 while Tegl can be considered to be uncemented and non-expanding soil allows the assumption  
419 that  $K_0$  is not affected.

## 420 **6. Conclusions**

421 The thickness of erosion of Brno Tegl was determined using three independent methods:  
422 Baldwin – Butler's equation, Casagrande's method and the geotechnical numerical back  
423 analysis.

424

425 1. According to Baldwin–Butler's equation the thickness of erosion corresponds to approx. 180  
426 – 270 m. The interval stems from the range of porosities (solidities) of undisturbed specimens  
427 as obtained from the oedometer tests.

428

429 2. Baldwin–Butler's equation has several deficiencies. Changes in porosity (solidity) due to  
430 unloading by erosion and/or reloading by further overburden are not captured. More  
431 importantly, it cannot allow for secondary compression, or the influence of other ageing effects.  
432 Moreover, Eq. (1) is created as a regression curve of collected data but these are in significant  
433 scatter and the equation is inaccurate in principle. These facts invalidate the estimations of the  
434 thickness of eroded layer using this method.

435

436 3. Casagrande's method yielded the thickness of erosion in the interval from 130 to 770 m. The  
437 effect of ageing was tackled using the coefficient of secondary compression, which however  
438 must be based on laboratory data at the time scale completely different from the geological  
439 times. However, further effects of ageing, probably related to chemo-structural changes, are  
440 also likely to affect the compressibility of the clay in the laboratory oedometer tests needed for  
441 Casagrande's method. It is possible to conclude that the method is not capable of determining  
442 the erosion thickness of the overconsolidated Brno Tegl.

443

444 4. The geotechnical numerical back analysis combined with the empirical dependence of  
445 horizontal *in-situ* stress (or  $K_0$ ) on *OCR* (true overconsolidation ratio) has the advantage of not  
446 having to deal with ageing.

447

448 5. The numerical model and the monitored mechanical behaviour around unsupported circular  
449 adits were found by  $K_0$  optimisation. From the resulting value of the earth pressure coefficient  
450 at rest  $K$  the thickness of erosion was estimated to be in the range from 0 to 40 metres, the most  
451 probable values being 20 to 40 metres.

452

453 6. The proposed combination of a numerical model of a thoroughly monitored excavation and  
454 the empirical equation by Mayne and Kulhawy (1982) proved a suitable tool for studying the  
455 erosion of aged sediments elsewhere in the Carpathian Foredeep, or at other sedimentary basins.

## 456 **7. Acknowledgements**

457 The authors thank to the grants [14-32105S]; and [15-05935S] of the Czech Science Foundation

458 .

459

## 460 **8. References**

461 Atkinson, J.H., 2007. The mechanics of soils and foundations. Taylor and Francis.



- 462 Baldwin, B., 1971. Ways of deciphering compacted sediments. *Journal of Sedimentary*  
463 *Research*, 41, 1
- 464 Baldwin, B., and Butler, C. O., 1985. Compaction curves. *AAPG bulletin*, 69, 4, 622-626.
- 465 Bjerrum, L., 1967. Engineering geology of Norwegian normally consolidated marine clays as  
466 related to settlements of buildings , 7th Rankine Lecture. *Geotechnique*, 17, 2, 81–118
- 467 Boháč, J., 1999. Pevnost a přetváření brněnského téglu , Strength and deformations of Brno  
468 Clay - in Czech. XI. Int. Scientific Conference, Technical University VUT, Brno, 33-36.
- 469 Boháč, J. a Pavlová, M., 2012. Předdenudační mocnost a překonsolidace brněnského téglu ,  
470 Overburden thickness and overconsolidation of Brno Tegel – in Czech. *Geotechnika*, 1+2,  
471 2012, 26-30.
- 472 Boháč, J., Mašín, D., Malát, R., Novák, V. and Rott, J., 2013. Methods of determination of  
473  $K_0$  in overconsolidated clay. In *Proceedings of the 18th International Conference ICSMGE*;  
474 Delage, P., Desrues, J. Frank, R. Puech, A. and Schlosser, F., Eds., Paris, France; Vol. 1, 203-  
475 206.
- 476 Bosák, P., Pruner, P., 2014. Magnetostratigrafie bádenských téglů z vrtu V1 Brno – Slatina ,  
477 Magnetostratigraphy of Badenian clays in Brno – Slatina – in Czech. Geological institute  
478 AVČR, 33 p.
- 479 Brooker, E.W., and Ireland, H. O., 1965. Earth pressures at rest related to stress history.  
480 *Canadian Geotechnical Journal*, 2, 1-15.
- 481 Brzobohatý, R., 1982. Rybí fauna spodnobádenských vápňitých jílu v Brně–Královo Poli a  
482 její paleogeografický význam., Lower-badenian fauna buried in lime clays in Brno - Královo  
483 pole and its relevance - in Czech *Časopis Moravského Muzea, Vědy přírodní*, 62, 57-64.
- 484 Burland, J. B., 1990. On the compressibility and shear strength of natural clays.  
485 *Géotechnique*, 40, 3, 329-378.
- 486 Casagrande, A., 1936. The Determination of the Pre-Consolidation Load and Its Practical  
487 Significance, *Proceedings of the 1st International Conference on Soil Mechanics and*  
488 *Foundation Engineering*, Paper D-34, Vol III, 60-34.
- 489 Chandler, R. J., 2010. Stiff sedimentary clays: geological origins and engineering properties.  
490 *Géotechnique*, 60, 12, 891-902.
- 491 Gareau, L. F., Molenkamp, F. and Sharma, J., 2006. An improved oedometer apparatus to  
492 measure lateral stress during testing. *Geotechnical Testing Journal*, 29, 3, 1–7.
- 493 Head, K.H. and Epps, R., 2011. *Manual of soil laboratory testing*, Vol. 2, 3rd ed., Whittles  
494 Publishing, 499pp.
- 495 Hight, D.W., McMillan, F., Powell, J.J.M., Jardine, R.J. and Allenou, C.P., 2003. Some  
496 characteristics of London Clay. *Proc. Characterisation and Engineering Properties of Natural*  
497 *Soils – Tan et al., eds. Swets and Zeitlinger*, 851-907.
- 498 Holz, R.D., and Jamiolkowski, M.B., 1985 Time dependence of lateral earth pressure. *Journal*  
499 *of geotechnical engineering*, 1239-1242.

500 Jefferies, M. G., Crooks, J. H. A., Becker, D. E., & Hill, P. R., 1987. Independence of  
501 geostatic stress from overconsolidation in some Beaufort Sea clays. *Canadian Geotechnical*  
502 *Journal*, 24, 3, 342-356.

503 Kavazanjian Jr, E. and Mitchell, J. K., 1984. Time dependence of lateral earth pressure.  
504 *Journal of Geotechnical Engineering*, 110, 4, 530-533.

505 Leonards, G. A., and Altschaeffl, A. G., 1964. Compressibility of clay. *Journal of the Soil*  
506 *Mechanics and Foundations Division*, 90, 5, 133-156.

507 Malát, R., Vilhelm, J., Rott, J. and Krupička, M., 2015. Horizontal stiffness of Brno clay  
508 measured by seismic cross-hole method, 6th International Geosciences Student Conference,  
509 13 – 16 July 2015, Prague, Czech republic , poster.

510 Mašín, D., 2005. A hypoplastic constitutive model for clays. *International Journal for*  
511 *Numerical and Analytical Methods in Geomechanics*, 29, 4, 311-336.

512 Mašín, D., 2014. Clay hypoplasticity model including stiffness anisotropy. *Géotechnique*, 64,  
513 3, 232-238.

514 Mašín, D. and Rott, J., 2014. Small strain stiffness anisotropy of natural sedimentary clays:  
515 review and a model. *Acta Geotechnica*, 9, 2, 299-312.

516 Mayne, P. W., and Kulhawy, F. H., 1982.  $K_0$ /OCR relationships in soil. *Journal of the*  
517 *Geotechnical Engineering Division*, 108, 6, 851-872.

518 Mesri, G. and Hayat, T.M., 1993. The coefficient of earth pressure at rest. *Canadian*  
519 *Geotechnical Journal*, 30, 4, 647-666.

520 Nehyba, S., 1997. Miocene volcanoclastics of the Carpathian Foredeep in the Czech  
521 Republic., *Věstník Českého geologického Ústavu* 72, 4, 311-327.

522 Pavlík, J., Klímek, L. and Rupp, D., 2004. Geotechnical exploration for the Dobrovského  
523 Tunnel, the most significant structure on the large city ring road in Brno , in Czech and  
524 English. *Tunel*, 13, 2, 2-12

525 Rott, J., 2014. Homogenisation and modification of composite steel-concrete lining, with the  
526 modulus of elasticity of sprayed concrete growing with time. *Tunel*, 23, 3, 53–60.

527 Rott, J. and Mašín, D., 2014. The FEM back-analysis of earth pressure coefficient at rest in  
528 Brno clay  $K_0$  with the homogenization of steel/shotcrete lining. In *Proceedings of the 25th*  
529 *Internatiopnal Conference Underground Infrastructure in Urban Areas 2014 , UIUA 2014*,  
530 Wroclaw, Poland; Madryas, C et al., Eds., Taylor and Francis Group; 113-124.

531 Rott, J., Mašín, D., Boháč, J., Krupička, M. and Mohyla, T., 2015. Evaluation of  $K_0$  in stiff  
532 clay by back-analysis of convergence measurements from unsupported cylindrical cavity.  
533 *Acta Geotechnica* 10, 6, 719-733.

534 Stráník, Z., Adámek, J., Brzobohatý, R., Buchta, Š., Dudek, A., Grygar, R., Otava, J.,  
535 Pálenský, P. and Tyráček, J.† , 2016 in press. *Geology of the Carpathians and SE margin of*  
536 *the West European platform in the Czech Republic*. Czech Geological Survey, Prague.

537 Svoboda, T., Mašín, D. and Boháč, J., 2009. Hypoplastic and Mohr-Coulomb models in  
538 simulations of a tunnel in clay , in Czech and English. *Tunel*, 18, 4, 59-68.

539 Svoboda, T., Mašín, D. and Boháč, J., 2010. Class A predictions of a NATM tunnel in stiff  
540 clay. *Computers and Geotechnics*, 37, 6, 817-825.